

The proton ladder, a static mechanism for ion/proton coports and counterports

D. T. Edmonds and R. Berry

The Clarendon Laboratory, Parks Road, Oxford OX1 3PU, United Kingdom

Received April 18, 1991 / Accepted in revised form August 2, 1991

Abstract. An ion/proton counterport is formed simply by locating a chain of ionizable residues connected by a proton conducting path near a passive ion pore which spans the membrane. The electric coupling between the ion in transit through the pore and the residues can ensure that for each ion passing through the pore in one direction a proton is driven along the chain of ionizable residues (the proton ladder) in the same or in the opposite direction. The mechanism is symmetrical in that a trans-membrane ion gradient may drive protons against their electro-chemical potential gradient or a proton gradient may drive ions against theirs. The mechanism is applicable to cation or anion channels and to coports or counterports. No mechanical motion is required other than the motion of the ions and the protons. Monte Carlo computer simulations are performed on the model and its predicted properties are listed. The new type of counterport model is compared with currently used models.

Key words: Ion/proton counterport – Model counterport

Introduction

Ion/proton counterports and coports form an essential component of living cells which allows them to convert a proton gradient into an ion gradient and vice versa (Mitchell 1985). Examples are the Na^+/H^+ counterport found in many preparations (Grinstein and Rothstein 1986), the K^+/H^+ counterport in mitochondria (Bernardi and Azzone 1983) or the K^+/H^+ coport in *Neurospora* (Blatt and Slayman 1987). Probably because of the 1:1 stoichiometry found experimentally, the models used to represent coports and counterports have usually been binding cavities which are exposed first to one side of the membrane and then the other (Jardetsky 1966; Vidavav 1966) or shuttling ionophores. Here we show that a counterport may be realized without any mechanical motion

simply by locating a chain of ionizable acid residues connected by a proton conducting path near a passive cation pore. The electrostatic coupling between the residues and ions in the pore will ensure that for each ion that passes through the pore in one direction, a proton is driven along the chain of sites (the proton ladder) in an anti-parallel direction. The system is symmetric in that a trans-membrane ion gradient may drive protons against their electro-chemical potential gradient or a proton gradient may drive ions against theirs. The mechanism is applicable to cation or anion pores and to coports or counterport but for definiteness only a cation/proton counterport will be discussed here.

The mechanism

The mechanism is most simply understood by considering a short cation channel spanning a membrane with two acid residues in its vicinity as sketched in Fig. 1 a. The residues are connected by a proton conducting path as indicated by the zig-zag line. The residues become negatively charged by losing a proton and neutral by binding one. The state of charge of the two residues may be represented by (1, 0) when only the left-hand residue is charged, by (0, 1) when only the right-hand residue is charged and by (0, 0) and (1, 1) when neither or both are charged. The connections between the various possible states of the two residues are shown as a kinetic diagram in Fig. 1 b. The diagonal transitions require the exchange of a proton with the fluids bathing the membrane faces while the equatorial transition represents the direct transfer of a proton between the two residues. When an ion occupies the channel, the proton transition rate constants in this diagram will depend on its position because of the electric field of the ion at the two residues.

In turn the energy profile of an ion traversing the channel will depend upon the state of charge of the residues and in Fig. 1 c are sketched these energy profiles for the 4 residue charge states. The major barrier for a small ion entering a narrow channel is the steep rise in electrostatic

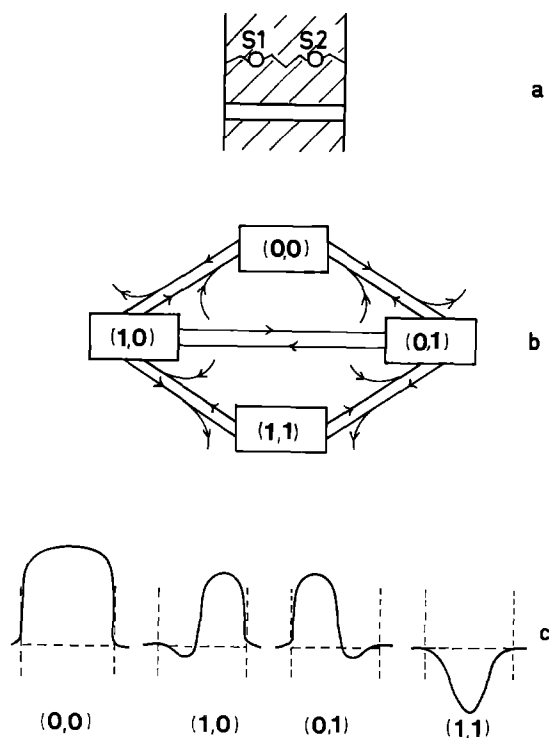


Fig. 1. **a** A sketch of two acid residues $S1$ and $S2$ situated near a trans-membrane ion pore. **b** The kinetic diagram giving the various transitions between the four possible charged states of the two acid residues. **c** The energy profiles experienced by a univalent cation traversing the channel in each of the four charged states of the acid residues, when no membrane voltage is applied. The ion energies are given relative to that in the aqueous fluid at either side of the channel

self-energy relative to its hydrated state (Parsegian 1969). This barrier, shown for the state (0, 0) is sufficient to prevent ion entry. However in the state (1, 0), the favourable interaction between the negatively charged residue and the cation, ensures that the left hand end of the pore forms an attractive binding site for cations while the barrier at the right hand end ensures that no ion can traverse the channel. Similarly the residue state (0, 1) allows ion entry from the right but no traverse.

To simulate a counterport the state (1, 1) is made unlikely by placing the residues sufficiently close together so that the doubly charged state has a high energy (Edmonds 1989). This effectively reduces Fig. 1 b to its upper triangle connecting the states (0, 0) to (1, 0) and (0, 1). By fixing the effective pK values of the residues to be greater than the prevailing pH , they rest predominantly in the state (0, 0) but with some probability of being in the states (1, 0) and (0, 1). Let us assume that, having rested in the state (0, 0), the channel state changes to (1, 0). In this state ion entry is possible from the left. Because of the electric interaction between the ion and the leftmost residue, this state is effectively locked-in. It will persist until the ion either leaves the channel on the left or moves toward the second residue. Such a move increases the probability of the state (0, 1) and the system may move toward another stable configuration with the ion in the right half of the channel and the site state (0, 1). This state is also locked-in until the ion moves back toward the first site or it leaves

the channel on the right. If the ion leaves, the residue state is free to return to the resting state (0, 0). Such a sequence corresponds to traversing the upper triangle of Fig. 1 b in a counter-clockwise direction and results in the transfer of a single ion from the left to right and a single proton from right to left as required in a counterport.

The channel may be made highly selective by adjusting the separation of the residues from the pore due to the steep dependence on ionic radius of the ionic electrostatic self-energy. As an example, consider the pore to be a single chain of water molecules of radius 0.14 nm. Larger ions are then excluded sterically. Let the residues be positioned at a distance from the pore such that a K^+ ion (radius 0.13 nm) has its self-energy within the narrow pore just cancelled by the favourable interaction with the negatively charged residue as sketched in Fig. 1c. Then smaller ions such as Na^+ (radius 0.095 nm) with a much larger self-energy will still be effectively excluded from the pore by the large energy barrier that remains even when the residue is charged. A sharp peak in probability of entry for cations of the target radius of 0.13 nm over that for cations of larger or smaller radius results. All anions of any radius will face a very high barrier to entry as the interaction with the acid residues adds to rather than subtracts from their self-energy while within the pore.

Simulation

These qualitative conclusions may be verified by a Monte Carlo computer simulation. To present it in its simplest form the continuous path of the ion may be replaced by 5 steps labelled by NI in Fig. 2a. Step 1 is in the left-hand fluid, step 5 in the right-hand fluid and steps 2, 3 and 4 within the pore and equally spaced across the membrane. The two acid residues within the membrane were assumed to have $pK = 8.5$ in the absence of applied voltages. They could consist of glutamic acid residues with their pK raised by 3 units owing to the low electrical polarizability of their surroundings when buried in the membrane (Edmonds 1989). They were disposed across the membrane such that $1/2$ the membrane voltage was dropped between the two residues and $1/4$ between each residue and the neighbouring membrane face. The electrical interaction energies between ion and residues may be written $U(S1, S2, NI)$ where $(S1, S2)$ gives the charged state of the residues as in the text and NI labels the ion step as in Fig. 2a. The values used, expressed as multiples of kT are

$$U(1,0,2)=U(0,1,4)=-18; \quad U(0,1,2)=U(1,0,4)=-5 \\ U(1,0,3)=U(0,1,3)=-15$$

The self energy of the ions was assumed to be +15 and the interaction energy between the residues when both are charged was taken as +15. The counterport action does not depend critically on these parameters provided that the residue state (1, 0) allows easy ion entry from the left with no direct transfer while (0, 1) allows entry from the right with no transfer. Treating the membrane as a dielectric slab of width 12 Å would mean that the residues are situated about 6 Å from the channel thus allowing the

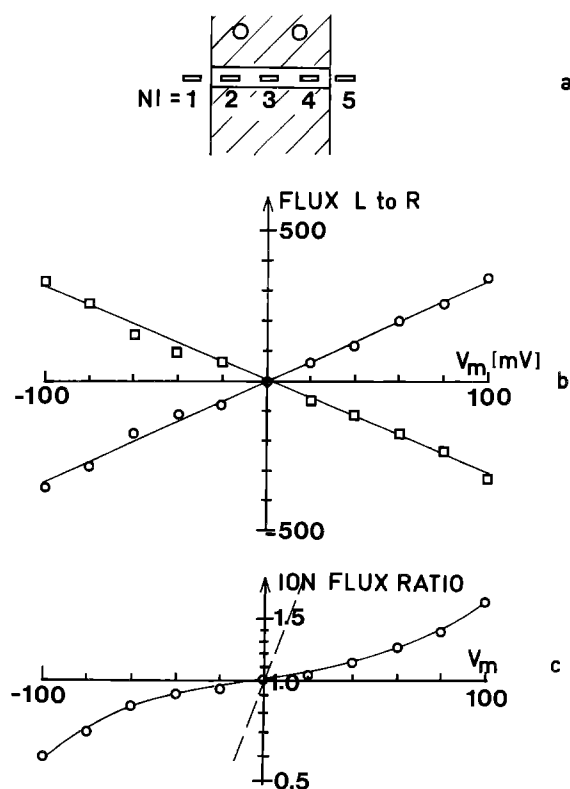


Fig. 2. **a** A simplified picture of the channel for easy computer simulation in which the continuous motion of the ion through the pore is broken into 5 discrete steps labelled by NI. **b** Prediction of the model for the left to right ion (○) and proton (□) fluxes in the absence of either an ion or a proton gradient across the membrane. The membrane voltage is the voltage on the left of the membrane less that on the right. The fluxes are those obtained for 10^6 ticks of the clock when averaged over 10^7 clock ticks. The number of ions moving down the membrane field gradient slightly exceeds the number of protons driven against the gradient so that the total energy falls. **c** A plot on a logarithmic scale of the ratio (ion flux left to right)/(ion flux right to left) as a function of membrane voltage in the absence of ion or proton gradients. The broken line gives the flux ratio expected for independent ion motion, namely $\exp(q \cdot V_m/kT)$ where q is the ion charge, V_m the membrane voltage, k the Boltzmann constant and $T=293$ K, the temperature

channel and sites to be separated by the diameter of an alpha-helix.

Proton kinetics are assumed fast so that for each ion position, the occupation probabilities of the various residue states in Fig. 1b rapidly reach a steady state which may be found analytically using partial diagrams (Hill 1966). With this knowledge, at each tick of the clock, a random number generator is consulted to determine the actual charged state of the residues. Knowing this and the interaction energies, the probabilities of ion entry or movement in the channel are known and then the actual move is decided by again consulting the random number generator. In such a model in which the residues and ions interact, it is the total energy of ion plus residues in a given configuration that determines its probability. A similar computer simulation for a passive channel with an adjacent switchable residue has been described before (Edmonds 1989).

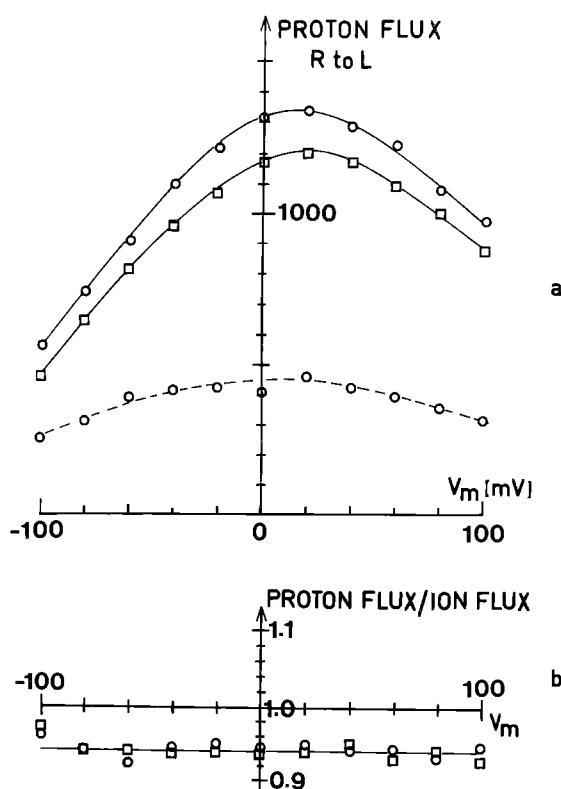


Fig. 3. **a** The proton flux from right to left in 10^6 clock ticks driven by a left to right ion concentration gradient of 100 : 1 (○) and 10 : 1 (□) with pH = 7 at both faces. At all positive membrane voltages, the protons are moving against their electro-chemical potential gradient. The broken line gives the equivalent proton flux for an ion gradient of 100 : 1 but when the protons are moving against a left to right proton gradient of 10 : 1 (pH = 6.5 : pH = 7.5). **b** The ratio of proton flux right to left to ion flux left to right when there is no proton gradient but an ion gradient left to right of 100 : 1 (○) and 10 : 1 (□). In both cases the stoichiometry is seen to remain slightly less than 1 with little dependence of the membrane voltage. All the model parameters remain as for Fig. 2

Results

Figure 2b shows the tight coupling between the ion and proton fluxes in response to a trans-membrane voltage when there are no ion or proton gradients across the membrane. Here the main driving force is the membrane field acting on the ion as it moves between the sites, thus allowing a change in the residue state. Figure 2c compares the ratio of the calculated unidirectional ion fluxes with the flux ratio expected for independent ion motion. A flux ratio close to 1 such as this is often taken as experimental evidence of a carrier rather than a pore.

Figure 3a illustrates the action of the model counterport in using a favourable ion gradient to drive protons against their electro-chemical gradient while Fig. 4a shows the same counterport acting in reverse, using a proton gradient to drive ions against their electro-chemical gradient. Figure 3b and 4b show that the ratio (pro-

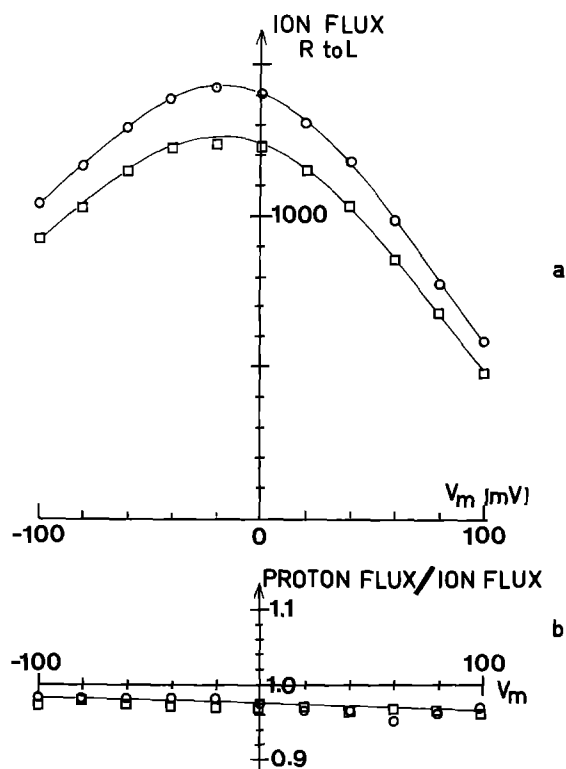


Fig. 4. **a** The same counterport operating in reverse with no ion gradient but with a left to right proton gradient of 100:1 (\circ) and 10:1 (\square) showing the flux of ions driven right to left in 10^6 clock ticks. **b** The ratio of proton flux to ion flux again shows a stoichiometry ratio close to 1 with little dependence on membrane voltage

ton flux/ion flux) is a little less than 1 and hardly varies with membrane voltage.

Comparison with previous models

The two most commonly used models for coports and counterports or indeed ATP driven pumps are the alternating access cavity (Jardetsky 1966; Vidavar 1966) and an ionophore shuttling across the membrane. The alternating access cavity is supposed to expose a cavity in the membrane protein alternatively to the outside and inside of the membrane. When exposed to the outside, a binding site within the cavity has a high affinity for ions of type A and a low affinity for type B. On switching access to the inside, the affinity of the binding site changes to having a high affinity for B and a low affinity for A. By alternating between these two configurations, type A ions are conveyed from outside to inside and type B from inside to outside. The model is useful as a teaching aid in graphically drawing attention to the changes in both affinity and access and may approximate to the real structure of transporters of larger molecules such as sugars. However, what is known of the molecular structure of the membrane spanning phase of ion exchange pumps (Maclennan et al. 1985; Ovchinnikov 1987) resembles that of passive ion channels. This is thought to consist of parallel bundle of alpha-helices and gives no support to a model

requiring alternating hydrophilic cavities. The shuttling ionophore does exist, for example as the bacterial antibiotic valinomycin, but again the structure of the membrane phase does not support such a model as an ion counterport or an ion pump.

An alternative type of model for an ion counterport (Edmonds 1986) consists of two distinct and selective ion channels coupled electrically. The present model falls into this category. It has the attractive property that it could have evolved from the chance juxtaposition of two passive ion channels. These models differ from the two above in that the two transfers occur simultaneously rather than sequentially. As a result they are electrically silent and require no energy storage.

The present model may be thought of as an alternating cavity model in which access is controlled electrically rather than mechanically. Although no specific ion binding site exists in the usual sense, the end of the pore adjacent to a residue that is charged forms a region with high affinity for particular ions as may be seen in Fig. 1c. The back reaction of the ion on the state of charge of the residues automatically provides the tight coupling between ion and proton motion required for an efficient counterport. Clearly a cation/cation coport or counterport may be visualized in a similar manner to the cation/proton counterport described here by allowing two adjacent and selective cation pores to interact with a common set of ionizable residues which change their charge in response to the electric fields of the transient ions.

The present model emerged from a study of the effects of allowing the electric structure of an ion channel to react (Edmonds 1989) to the large electric field of an ion in transit. Besides the coports and counterports described here, if the motion of ions passing through two adjacent but identical pores is correlated by interacting with a common set of ionizable residues, a related model of a "multi-ion" pore such as the delayed rectifier potassium channel is obtained. This work will be presented elsewhere.

Predicted properties of the model

Below are listed some of the predicted properties of this model of an ion/proton counterport which can be tested experimentally.

- (1) The counterport is fast with a maximum transfer rate comparable with a passive ion channel of about 10^6 /s.
- (2) The unidirectional transfer rate as a function of ion concentration will obey simple Michaelis-Menten kinetics as only a single binding site (the pore mouth) is involved.
- (3) The pH dependence is more complicated as this affects not only the number of protons available for transit but also the resting state of charge of the residues. With a symmetrical pH of 5 there is negligible transfer even with plentiful ions and 100 mV across the membrane, because the resting state is then predominantly (0, 0) which allows no flow of ions or protons. The simple two-site model described predicts leakage of ions in the absence of protons (pH = 10) as the (0, 1) and (1, 0) states

become dominant in the resting state. This leakage can be eliminated in more complex models.

(4) The stoichiometric ratio does not depend upon membrane voltage as shown in the figures. The membrane voltage dependence of the transfer rate is appreciable when the counterport is idling (full lines in Fig. 3a) but becomes much less when transferring protons against an adverse proton gradient (broken line in Fig. 3a).

(5) The device is electrically silent as both transfers occur together. However in the absence of ions the charge (proton) transfer that occurs when the counterport changes between the possible resting states of (0, 0), (0, 1) and (1, 0) should be detectable (Edmonds 1990) by measuring changes in the effective capacitance of a membrane containing them.

References

- Bernardi P, Azzone GF (1983) Electroneutral H^+/K^+ exchange in liver mitochondria. Regulation by membrane potential. *Biochim Biophys Acta* 724:212–223
- Blatt MR, Slayman CL (1987) Role of active potassium transport in the regulation of cytoplasmic pH by nonanimal cells. *Proc Natl Acad Sci* 84:2737–2741
- Edmonds DT (1986) A two-channel electrostatic model of an ionic counterport. *Proc R Soc B* 228:71–84
- Edmonds DT (1989) A kinetic role for ionizable sites in membrane channel proteins. *Eur Biophys J* 17:113–119
- Edmonds DT (1990) Gating charge transfer due to fixed ionizable sites. *Eur Biophys J* 18:135–137
- Grinstein S, Rothstein A (1986) Mechanisms of regulation of the Na^+/H^+ exchanger. *J Memb Biol* 90:1–12
- Hill TL (1966) Studies in irreversible thermodynamics (IV) Diagrammatic representation of steady state fluxes for unimolecular systems. *J Theor Biol* 10:442–459
- Jardetsky O (1966) Simple allosteric model for membrane pumps. *Nature* 211:969–970
- Mitchell P (1985) The correlation of chemical and osmotic forces in biochemistry. *J Biochem* 97:1–18
- MacLennan DH, Brandl CJ, Korczak B, Green NM (1985) Amino acid sequence of a $Ca^{++}Mg^{++}$ -dependent ATPase from rabbit muscle sarcoplasmic reticulum, deduced from its complementary DNA sequence. *Nature* 316:696–700
- Ovchinnikov YA (1987) Probing the folding of membrane proteins. *Trends Biol Sci* 12:434–438
- Parsegian VA (1969) Energy of an ion crossing a low dielectric membrane: solutions of four relevant problems. *Nature* 221:844–846
- Vidavav GA (1966) Inhibition of parallel flux and augmentation of counterflux shown by transport models not involving a mobile carrier. *J Theor Biol* 10:301–306